doi:10.1093/brain/aww010 BRAIN 2016: 139; 1282–1294 | 1282

BRAIN
A JOURNAL OF NEUROLOGY

Neural substrates of vulnerability to postsurgical delirium as revealed by presurgical diffusion MRI

Michele Cavallari,[1] Weiying Dai,[2,3] Charles R. G. Guttmann,[1] Dominik S. Meier,[1] Long H. Ngo,[4] Tammy T. Hshieh,[5,6] Amy E. Callahan,[2] Tamara G. Fong,[6,7] Eva Schmitt,[6] Bradford C. Dickerson,[8,9,10] Daniel Z. Press,[7] Edward R. Marcantonio,[4] Richard N. Jones,[11] Sharon K. Inouye[4,6,*] and David C. Alsop[2,*] on behalf of the SAGES Study Group

[*]These authors contributed equally to this work.

Despite the significant impact of postoperative delirium on surgical outcomes and the long-term prognosis of older patients, its neural basis has not yet been clarified. In this study we investigated the impact of premorbid brain microstructural integrity, as measured by diffusion tensor imaging before surgery, on postoperative delirium incidence and severity, as well as the relationship among presurgical cognitive performance, diffusion tensor imaging abnormalities and postoperative delirium. Presurgical diffusion tensor imaging scans of 136 older ($\geqslant$70 years), dementia-free subjects from the prospective Successful Aging after Elective Surgery study were analysed blind to the clinical data and delirium status. Primary outcomes were postoperative delirium incidence and severity during the hospital stay, as assessed by the Confusion Assessment Method. We measured cognition before surgery using general cognitive performance, a composite score based on a battery of neuropsychological tests. We investigated the association between presurgical diffusion tensor imaging parameters of brain microstructural integrity (i.e. fractional anisotropy, axial, mean and radial diffusivity) with postoperative delirium incidence and severity. Analyses were adjusted for the following potential confounders: age, gender, vascular comorbidity status, and general cognitive performance. Postoperative delirium occurred in 29 of 136 subjects (21%) during hospitalization. Presurgical diffusion tensor imaging abnormalities of the cerebellum, cingulum, corpus callosum, internal capsule, thalamus, basal forebrain, occipital, parietal and temporal lobes, including the hippocampus, were associated with delirium incidence and severity, after controlling for age, gender and vascular comorbidities. After further controlling for general cognitive performance, diffusion tensor imaging abnormalities of the cerebellum, hippocampus, thalamus and basal forebrain still remained associated with delirium incidence and severity. This study raises the intriguing possibility that structural dysconnectivity involving interhemispheric and fronto-thalamo-cerebellar networks, as well as microstructural changes of structures involved in limbic and memory functions predispose to delirium under the stress of surgery. While the diffusion tensor imaging abnormalities observed in the corpus callosum, cingulum, and temporal lobe likely constitute the neural substrate for the association between premorbid cognition, as measured by general cognitive performance, and postoperative delirium, the microstructural changes observed in the cerebellum, hippocampus, thalamus and basal forebrain seem to constitute a separate phenomenon that predisposes to postsurgical delirium independent of presurgical cognitive status.

1 Center for Neurological Imaging, Department of Radiology, Brigham and Women's Hospital, Harvard Medical School, Boston, MA, USA
2 Department of Radiology, Beth Israel Deaconess Medical Center, Harvard Medical School, Boston, MA, USA
3 Department of Computer Science, State University of New York at Binghamton, Binghamton, NY, USA
4 Department of Medicine, Beth Israel Deaconess Medical Center, Harvard Medical School
5 Division of Aging, Brigham and Women's Hospital, Harvard Medical School, Boston, MA, USA
6 Aging Brain Center, Institute for Aging Research, Hebrew SeniorLife, Boston, MA, USA

Received October 01, 2015. Revised December 07, 2015. Accepted December 16, 2015. Advance Access publication February 26, 2016

7 Department of Neurology, Beth Israel Deaconess Medical Center, Harvard Medical School, Boston, MA, USA
8 Martinos Center for Biomedical Imaging, Massachusetts General Hospital and Harvard Medical School, 149 13th St., Charlestown, MA, USA
9 Psychiatric Neuroimaging Division, Department of Psychiatry, Massachusetts General Hospital and Harvard Medical School, 149 13th St., Charlestown, MA, USA
10 Frontotemporal Disorders Unit, Department of Neurology, Massachusetts General Hospital and Harvard Medical School, 149 13th St., Charlestown, MA, USA
11 Departments of Psychiatry and Human Behavior and Neurology, Brown University Warren Alpert Medical School, Providence, RI, USA

Correspondence to: David C. Alsop, PhD,
Department of Radiology,
Ansin 226, Beth Israel Deaconess Med Ctr,
330 Brookline Avenue, Boston MA 02215,
USA
E-mail: dalsop@bidmc.harvard.edu

Keywords: delirium; temporal lobe; structural MRI; cognitive ageing; neuropsychiatry

Abbreviations: CAM = confusion assessment method; DTI = diffusion tensor imaging; GCP = general cognitive performance; SAGES = Successful Aging after Elective Surgery; SPM = Statistical Parametric Mapping; TRACULA = tracts constrained by underlying anatomy

Introduction

Postoperative delirium (also known as acute confusional state or toxic metabolic encephalopathy) is one of the most frequent complications of surgical procedures in hospitalized patients over 65 years old, with an incidence ranging from 11% to as much as 51% (Inouye *et al.*, 2014). Although the attention deficits and cognitive impairment distinctive of delirium episodes are usually transient, delirium can have disabling and permanent sequelae. Patients with postoperative delirium showed doubled rehospitalization rates and quadrupled mortality rates compared to patients without delirium (Marcantonio *et al.*, 2005). Their trajectories of functional and cognitive deterioration showed faster decline compared to their non-delirious counterparts (Quinlan and Rudolph, 2011; Saczynski *et al.*, 2012). Although delirium constitutes a life-threatening syndrome, it is preventable in 30–40% of cases through interventions targeting predisposing and precipitating factors (Inouye *et al.*, 1999; Marcantonio *et al.*, 2001; Milisen *et al.*, 2001). The prevention and treatment of delirium remain challenging because the aetiology of delirium is multifactorial and its pathogenesis poorly understood. Major precipitating and predisposing factors of delirium include medical conditions that perturb brain homeostasis by altering its structure and/or function, including dementia, cerebrovascular diseases, depression, infections, and psychoactive drugs (Inouye *et al.*, 2014).

To advance understanding of the pathogenesis of delirium, recent neuroimaging studies aimed to characterize the neuroanatomical substrate of delirium and its predisposing factors, by measuring quantitative indices of brain pathology, such as global and regional atrophy, and white matter hyperintensity volume (Alsop *et al.*, 2006; Gunther *et al.*, 2012; Hatano *et al.*, 2013; Root *et al.*, 2013; Cavallari *et al.*, 2015). Further elucidation of neuroimaging biomarkers predictive of delirium theoretically would allow clinicians to emphasize preventive strategies in subjects with high-risk profiles, and ultimately contribute to understanding the intricate, multifactorial pathogenesis of delirium.

The results of previous neuroimaging studies are inconsistent. Although some studies suggested that brain atrophy and white matter abnormalities are associated with delirium (Alsop *et al.*, 2006; Gunther *et al.*, 2012; Hatano *et al.*, 2013; Root *et al.*, 2013), our prior work in a well-characterized cohort of dementia-free subjects with postoperative delirium assessed by MRI before surgery has not found any association of delirium incidence and severity with white matter hyperintensity volume, hippocampal or global brain atrophy (Cavallari *et al.*, 2015). While these measures of macroscopic structural brain damage were not associated with occurrence and severity of delirium, we were able to detect an inverse association of cognitive status, as measured by general cognitive performance (GCP) before surgery (Jones *et al.*, 2010), with postoperative delirium incidence and severity (Cavallari *et al.*, 2015). All of these findings together suggest that the observed association between GCP and delirium likely has a different substrate than macroscopic white matter damage and brain atrophy. It is conceivable that other MRI biomarkers of structural brain changes linked to variability in cognitive performance could be associated with delirium. We hypothesized that premorbid brain microstructural abnormalities as measured by DTI can predispose to delirium under the stress of surgery.

Diffusion tensor imaging (DTI) is an MRI technique that provides indices of microstructural integrity of the brain parenchyma, such as fractional anisotropy, axial diffusivity, mean diffusivity and radial diffusivity, by encoding the

diffusion dynamics of water molecules within the tissue (Pierpaoli *et al.*, 1996). DTI has been especially applied to measure structural brain connectivity, and to map regional microstructural damage to white matter fibre tracts underlying functional impairment in several conditions, including ageing, dementia and schizophrenia (Thomason and Thompson, 2011; Sasson *et al.*, 2012; Griffa *et al.*, 2013). Previous knowledge about DTI abnormalities in subjects with postoperative delirium is limited to two studies, which showed fractional anisotropy changes of the frontal white matter, thalamus, corpus callosum and internal capsule in subjects with delirium (Shioiri *et al.*, 2010; Morandi *et al.*, 2012).

In the present study, first we investigated the association of brain microstructural abnormalities, as assessed by DTI before surgery, with postoperative delirium incidence and severity in the same cohort of dementia-free older subjects undergoing elective surgery on which we reported previously (Cavallari *et al.*, 2015). Second, we investigated the relationship between DTI abnormalities, cognitive status and postoperative delirium. Specifically, by controlling for presurgical cognitive performance in secondary analysis, we aimed to differentiate those DTI abnormalities that represent the neuropathological correlate of the observed association between cognitive performance and delirium, from those independent from the baseline cognitive status.

Materials and methods

Study design and cohort assembly

Our study population is a subsample of the Successful Aging after Elective Surgery (SAGES) study, an ongoing prospective cohort study of older adults undergoing elective major non-cardiac surgery. The study design and methods have been described previously (Schmitt *et al.*, 2012). Briefly, eligible participants were age 70 years and older, English speaking, scheduled to undergo elective surgery at one of two Harvard-affiliated academic medical centres and with an anticipated length of stay of at least 3 days. Eligible surgical procedures were: total hip or knee replacement, lumbar, cervical, or sacral laminectomy, lower extremity arterial bypass surgery, open abdominal aortic aneurysm repair, and colectomy. Exclusion criteria included evidence of dementia, delirium, hospitalization within 3 months, terminal condition, legal blindness, severe deafness, history of schizophrenia or psychosis, and history of alcohol abuse. A total of 566 patients were enrolled between 18 June 2010 and 8 August 2013. A subset of approximately one-third of the enrolled SAGES study participants was recruited to undergo MRI 1 month before surgery ($n = 147$). Additional exclusion criteria for the nested cohort MRI study included contraindications to 3 T MRI (such as pacemakers, and certain stents and implants). Written informed consent was obtained from all participants according to procedures approved by the institutional review boards of Beth Israel Deaconess Medical Center and Brigham and Women's Hospital, the two study hospitals, and Hebrew SeniorLife, the study coordinating centre, all located in Boston, Massachusetts.

Outcome measures

The outcomes of interest were postoperative delirium incidence (dichotomous outcome) and delirium severity (continuous outcome) during the hospital stay. We used both the confusion assessment method (CAM) and a validated chart review method to detect delirium for each patient. If both, or either of the two methods indicated that the patient had delirium, then that patient was defined as having delirium. The CAM is a widely used, standardized method for identification of delirium that has high sensitivity, specificity and inter-rater reliability (Wei *et al.*, 2008), which is described in detail elsewhere (Inouye *et al.*, 1990). It is based on structured interviews, including formal cognitive testing, administered to patients daily during hospitalization by trained interviewers. The CAM diagnostic algorithm requires the presence of acute change or fluctuating course, inattention, and either disorganized thinking or an altered level of consciousness to fulfil criteria for delirium. The validated chart review method (Inouye *et al.*, 2005; Saczynski *et al.*, 2014) was performed to enhance sensitivity in detecting delirium episodes across each 24-h period, as the daily interview period with the CAM assessment was brief. The chart review method, based on search for key words and full text review of any episode of confusion or agitation, has been previously validated and is widely used. Each chart rating was adjudicated independently by two experts (geriatrician and neuropsychologist) according to prespecified criteria to determine possible, probable, definite delirium, or no delirium. Any discrepancies between the two reviewers were resolved during a consensus conference.

Delirium severity was assessed by the CAM-S Long Form, with scores ranging from 0 to 19 (19 = most severe) (Inouye *et al.*, 2014). Peak CAM-S scores were used in the analyses as a continuous measure of delirium severity.

Our primary analysis investigated the association of presurgical DTI abnormalities with postoperative delirium incidence and severity, controlling for age, gender and vascular comorbidities as potential confounders. In secondary analysis, presurgical GCP score was also used as a covariable to assess the independent association of DTI indices with delirium incidence and severity with respect to cognitive performance in a separate multivariate model (including age, gender and vascular comorbidity as additional covariables).

Covariables

The following variables were incorporated into our primary analysis to adjust for potential confounders: age, gender, and vascular comorbidity status. Age refers to the participant's age (years) at the time of surgery. The following conditions were considered to define vascular comorbidity: confirmed or history of myocardial infarction, congestive heart failure, peripheral vascular disease, diabetes (with or without end organ damage), cerebrovascular disease (carotid stenosis, history of stroke or transient ischaemic attack), or hemiplegia. The study subjects were categorized in two categories (with/without vascular comorbidity), according to the presence or absence of at least one of the pathological conditions mentioned above. It is important to note that we were parsimonious in our choice of covariables for analyses, as we wanted to adjust for important baseline covariables, yet avoid over-controlling for variables that might be intermediaries between the DTI parameters

and delirium (such as medications and hospitalization factors) (Glymour and Greenland, 2008; Schisterman *et al.*, 2009).

GCP score was used as a covariable in secondary analysis using a separate multivariate model (including age, gender and vascular comorbidity as additional covariables). Cognitive performance was assessed by a neuropsychological test battery administered before surgery. Median number of days between cognitive testing and MRI was 5 (interquartile range = 1–8). We measured cognition using the GCP, a weighted composite score based on the battery of neuropsychological tests administered to assess attention, memory, learning and executive functioning (Jones *et al.*, 2010). The battery includes the Hopkins Verbal Learning Test (Brandt, 1991), the Visual Search and Attention Task (Trenerry *et al.*, 1990), the Trail Making Tests A and B (Trail Making Tests A and B, 1944), the Digit Symbol Substitution and Copy tests (Wechsler, 1981), the Digit Span forward and backward (Wechsler, 1981), and the 15-item Boston Naming Test (Mack *et al.*, 1992). A higher GCP score indicates better cognitive performance. The GCP score in SAGES was scaled to reflect population-based norms (Gross *et al.*, 2014) with a mean value of 50 [standard deviation (SD) = 10]. Therefore, a change in 10 units on the mean GCP score corresponds to a difference in cognitive functioning that is 1 SD from the mean of the age-adjusted US population.

We also investigated the cross-sectional association of DTI indices with age and cognitive performance before surgery in separate, supplementary analysis. Analysis of the association between DTI indices and age refer to the general linear model used for our primary analysis (i.e. with delirium severity, gender and vascular comorbidities as covariables). Analysis of the association between DTI indices and GCP was adjusted for age, gender and years of education.

MRI acquisition

All subjects were imaged before surgery (median = 7, interquartile range = 4–13 days) at the Beth Israel Deaconess Medical Center Radiology Department on a 3 T HDxt MRI (General Electric Medical Systems) scanner using a standard 8-channel head coil. All participants completed a standard clinical screening form for MRI safety and contraindications before the MRI scan.

The complete MRI acquisition protocol included 3D anatomical T_1-weighted imaging, high-resolution 3D T_2-weighted imaging, 2D fluid-attenuated inversion recovery, and arterial spin labelling. Results of these image modalities are being analysed and reported separately (Cavallari *et al.*, 2015). The characteristics of the DTI image protocol were:

Echo planar diffusion-weighted imaging, using a double echo diffusion preparation sequence with repetition time = 16 000 ms, echo time = 84.4 ms, acquisition matrix = 96 × 96, flip angle = 90°, field of view = 240 × 240 mm, slice thickness = 2.6 mm and in plane resolution of 2.5 mm. Images were acquired with a b-value of 1000 s/mm^2 at each of 25 optimized diffusion directions.

DTI analysis

TRACULA (tracts constrained by underlying anatomy) in FreeSurfer 5.2 was used to preprocess the diffusion-weighted images, mitigate image distortions due to eddy currents and magnetic field inhomogeneities, perform skull-stripping, align the individual's diffusion-weighted and anatomical T_1-weighted images to one another, resample and align the diffusion images to the MNI space, and extract the eigenvectors and eigenvalues diffusion maps [i.e. lambda-1 (or axial diffusivity), lambda-2, lambda-3 maps]. The processing workflow of TRACULA is based on a standardized routine that utilizes tools available in the software library of FSL (http://fsl.fmrib.ox.ac.uk/fsl), and is described in detail elsewhere (Yendiki *et al.*, 2011; https://surfer.nmr.mgh.harvard.edu/fswiki/tracall). Briefly, mitigation of distortion due to eddy current and motion were obtained by registering the diffusion-weighted to the b = 0 images using FSL's eddy_correct. Magnetic field inhomogeneities were corrected using epidewarp.fsl. Skull-stripping was performed through FSL's bet. TRACULA used prior anatomical information derived from cortical parcellation and subcortical segmentation obtained for each subject by processing the individual T_1-weighted images through FreeSurfer (http://freesurfer.net/). The individual anatomical T_1-weighted images were aligned to the b = 0 images, and then to the 1 mm resolution MNI-152 atlas through affine registration using FSL's flirt. The diffusion maps were obtained by least-squares tensor estimation using FSL's dtifit. While axial diffusivity, fractional anisotropy and mean diffusivity maps were provided as output of TRACULA preprocessing, we obtained radial diffusivity maps by averaging the lambda-2 and lambda-3 maps. To improve alignment between individual diffusion maps and account for atrophy-related effects on registration (Keihaninejad *et al.*, 2013), we ran two iterations of a non-linear normalization routine in Statistical Parametric Mapping (SPM) 8 (http://www.fil.ion.ucl.ac.uk/spm) to align the individual resampled 1 × 1 × 1 mm fractional anisotropy maps to the average fractional anisotropy map obtained from individual fractional anisotropy maps in MNI coordinate space. Interindividual alignment between the other diffusion maps (i.e. axial-, mean- and radial diffusivity maps) was obtained using the transformation matrices obtained from normalization of the individual fractional anisotropy maps to the average fractional anisotropy maps. Accuracy of spatial normalization was assessed visually by the operators who performed the analysis by evaluating blurring of the ensemble mean, as well as alignment of anatomical brain structures between individual images and the ensemble mean, using the check registration function of SPM. The diffusion maps were then smoothed using a Gaussian kernel of 3 mm full width at half maximum, and voxel-wise analysis of the smoothed diffusion maps was performed using SPM8. General linear modelling was used to estimate the association of DTI values with delirium incidence and severity. Assumption of normality was assessed by analysing the histogram plots of the contrast images provided by SPM using vis (http://tools.robjellis.net). In our primary analysis, the following covariables were included in the model: age, gender, and vascular comorbidity. To assess the independent association between DTI parameters and delirium after adjusting for GCP, we performed secondary analysis also including GCP as a covariable in the model (in addition to age, gender and vascular comorbidity).

In supplementary analyses we assessed the association between DTI parameters and age (controlling for delirium severity, gender and vascular comorbidity), as well as between DTI parameters and GCP (controlling for age, gender and education).

We determined empirically that a one-tailed *P*-value threshold of 0.05 at the voxel level with cluster size of 5000 voxels or larger provided significant results (*P*-value $\leqslant 0.05$ after correction for multiple comparison within each cluster). In voxel-based structural MRI analysis (such as DTI) cluster-extent based correction for multiple comparisons (Friston *et al.*, 1994) is an established method to account for the number of statistical tests. This approach basically consists of two steps. First, an arbitrary voxel-level *P*-value threshold ($P = 0.05$ in our study) defined clusters by retaining those groups of voxels showing *P*-values below the set threshold when testing for the association between delirium and signal intensity of each voxel. Then, a cluster-level extent threshold, measured in numbers of contiguous voxels, was used to estimate and correct for the false positive probability (type 1 error) of the cluster region as a whole, under the null hypothesis of no association between delirium and signal intensity of any voxel of that cluster. This approach was applied to all the voxel-based analyses included in the manuscript.

We confirmed the features of the voxel-based analysis obtained through SPM with tract-based spatial statistics (TBSS) analysis using FSL. The results obtained through TBSS analysis were qualitatively similar to those obtained by SPM (data not shown).

We also explored the magnitude of the association between DTI abnormalities and delirium, by performing supplementary region of interest analysis. We measured the diffusion parameters of the whole cerebral white matter by using the individual white matter masks provided by TRACULA, obtained from the FreeSurfer cortical parcellation and subcortical segmentation. In addition, regions of interest were defined by extracting the clusters that showed significant association with delirium severity in voxel-wise analysis. The mean fractional anisotropy, and mean-, axial- and radial diffusivity values within the regions of interest were calculated using MarsBaR (Brett *et al.*, 2002). We reported and compared those DTI values in subjects who developed delirium and subjects who did not. In addition, regression analysis of the association between the DTI values of the regions of interest and delirium severity was performed, as explained in detail in the 'Statistical analysis' section below. Given the exploratory nature of this analysis, which was based on heuristic definition of the regions of interest rather than *a priori*, we reported the results as Supplementary material.

MRI analyses were performed by two operators (M.C., W.D.) blind to the demographic and clinical data, including delirium outcomes.

Statistical analysis

Student's *t*-test or Mann-Whitney test was used to assess differences in continuous variables between subjects who developed delirium and subjects who did not, according to the distribution of the data. Chi-square or Fisher's exact tests were used to assess differences in categorical variables between subjects who developed delirium and subjects who did not, as appropriate. General linear modelling was used to measure the association of DTI values with delirium incidence and severity in voxel-wise analysis using SPM8, as specified in the 'DTI analysis' section. JMP Pro version 11 (www.jmp.com) was used for statistical analysis of the demographic and clinical variables, as well as for the supplementary region of interest analysis. Specifically, group comparisons of the mean DTI indices of each region of interest between subjects with delirium and subjects with no delirium were assessed by two-sided Student's *t*-test. General linear model was used to measure the association between delirium severity (outcome measure) and the mean DTI values of the regions of interest (regressors), adjusting for age, gender and vascular comorbidity. Separate regression models for each region of interest were performed.

Table 1 Baseline characteristics of the study participants

	All subjects	Delirium	No delirium	*P*-value
Number of subjects	136	29	107	–
Age (years, mean ± SD)	76 ± 4	76 ± 4	76 ± 5	0.451[b]
Female gender (*n*, %)	80 (59%)	20 (69%)	60 (56%)	0.205[c]
Non-white or Hispanic (*n*, %)	12 (9%)	2 (7%)	10 (9%)	1.000[d]
Education (years, mean ± SD)	15 ± 3	14 ± 2	15 ± 3	0.147[b]
3MS Score (0–30, 0 most severe; mean ± SD)	26 ± 1	26 ± 2	27 ± 1	0.175[b]
GCP Score (externally scaled, mean ± SD)	58 ± 7	54 ± 7	59 ± 7	0.003[a]
Vascular comorbidity (*n*, %)	54 (40%)	12 (41%)	42 (39%)	0.836[c]
Surgery (*n*, %)				
Orthopaedic	113 (83%)	27 (93%)	86 (80%)	0.325[d]
Vascular	6 (4%)	0 (0%)	6 (6%)	
Gastrointestinal	17 (13%)	2 (7%)	15 (14%)	

P-values refer to group comparison no delirium versus delirium by:
[a]Student's *t*-test;
[b]Mann-Whitney test;
[c]Chi-Squared test; or
[d]Fisher's exact test
3MS = Modified Mini-Mental State Examination.

Results

Of 147 subjects who had MRI prior to surgery, 10 did not complete the DTI protocol, and therefore were excluded from this study. DTI failures primarily reflected participant inability to tolerate the duration of scan, as DTI was the final sequence of the MRI protocol. The TRACULA registration algorithm used to perform alignment of the DTI images failed in one subject due to the presence of expanded retrocerebellar CSF space associated with cerebellar atrophy, therefore the subject was not included in this study. Demographic and baseline clinical characteristics of the 136 subjects included in this study are summarized in Table 1. The subsample investigated in the present study presented no overall differences in the baseline characteristics with respect to the whole cohort of subjects who underwent MRI, on which we reported previously (Cavallari *et al.*, 2015). No significant differences in age, gender,

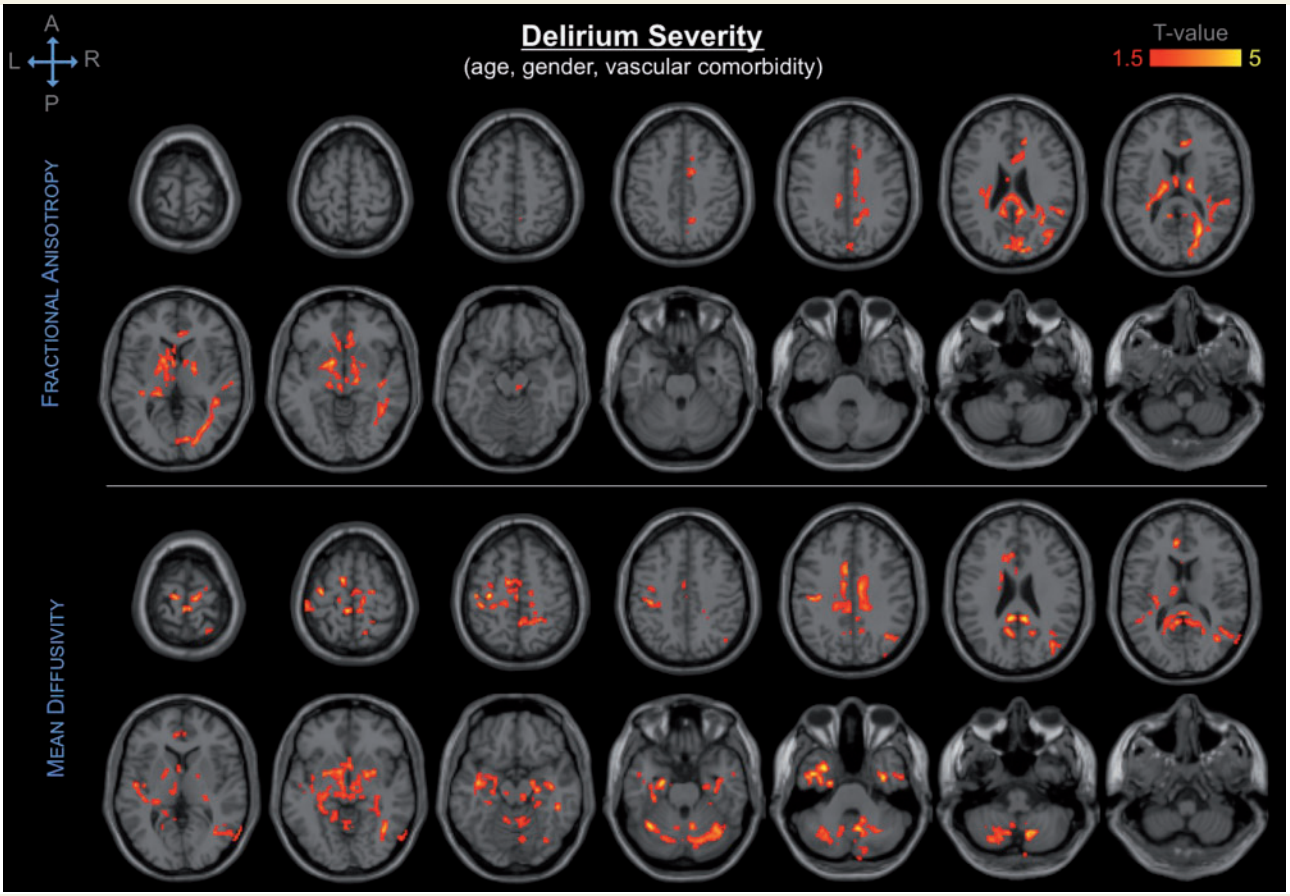

Figure 1 Spatial distribution and significance of association between DTI abnormalities and delirium severity, adjusting for age, gender and vascular comorbidity. Areas showing decrease in fractional anisotropy (*top*) and increase in mean diffusivity (*bottom*) are overlaid to canonical T_1-weighted images. Colours refer to T-values of significant DTI abnormalities ($P < 0.05$ after correction for multiple comparison within each cluster, cluster size $\geqslant 5000$) on a scale of 1.5 (red) to 5 (yellow).

education and vascular comorbidity were found between subjects with and without delirium. Subjects with delirium showed significantly lower GCP (Table 1).

Postoperative delirium occurred in 29 of 136 subjects (21%) during hospitalization. Delirium was diagnosed in 24 subjects by the CAM method, in five subjects by charts review. CAM-S scores were significantly higher in the delirium group compared to the group without delirium (mean $\pm$ SD = 8 ± 4 versus 2 ± 2; Mann-Whitney test, $P < 0.0001$).

The DTI findings showed significant association of presurgical DTI abnormalities—i.e. decreased fractional anisotropy, and increased axial-, mean- and radial diffusivity—in a variety of brain regions with postoperative delirium incidence and severity. Delirium severity was associated with a broader spatial pattern of DTI abnormalities as compared to that associated with delirium incidence. Our primary analysis of the association between presurgical DTI indices and postoperative delirium controlling for age, gender and vascular comorbidities, showed DTI abnormalities in the following structures: cerebellum, cingulum, corpus callosum, internal capsule, substantia innominata/basal forebrain, thalamus, occipital, parietal and temporal lobes, including the hippocampus (Fig. 1).

When controlling also for GCP (in addition to age, gender and vascular comorbidities), DTI abnormalities of the cerebellum, hippocampus, substantia innominata/basal forebrain, and thalamus still remained associated with delirium outcomes (Fig. 2).

Among those structures, DTI abnormalities of the cerebellum showed the most significant association with postoperative delirium. The observed cerebellar abnormalities mainly involved the vermis and neocerebellar structures, such as the posterior lobes and areas neighbouring the dentate nuclei and middle cerebellar peduncles. Thalamic DTI abnormalities involved the dorsomedial, ventromedial, and anterior portion of the thalamus, extending towards the internal capsule. Hippocampal abnormalities were observed bilaterally in the hippocampal head (as well as portions of the entorhinal and perirhinal cortices) and extended caudally in the dorsal hippocampal body/fimbria and along the left hippocampal tail in the fimbria and dorsally into the fornix, as well as in the subthalamic nucleus (Fig. 3). Prominent effects were also seen in the bilateral substantia innominata (basal forebrain) as well as the anterior commissure (Fig. 4).

When comparing visually the results obtained from different DTI indices, mean and radial diffusivity showed

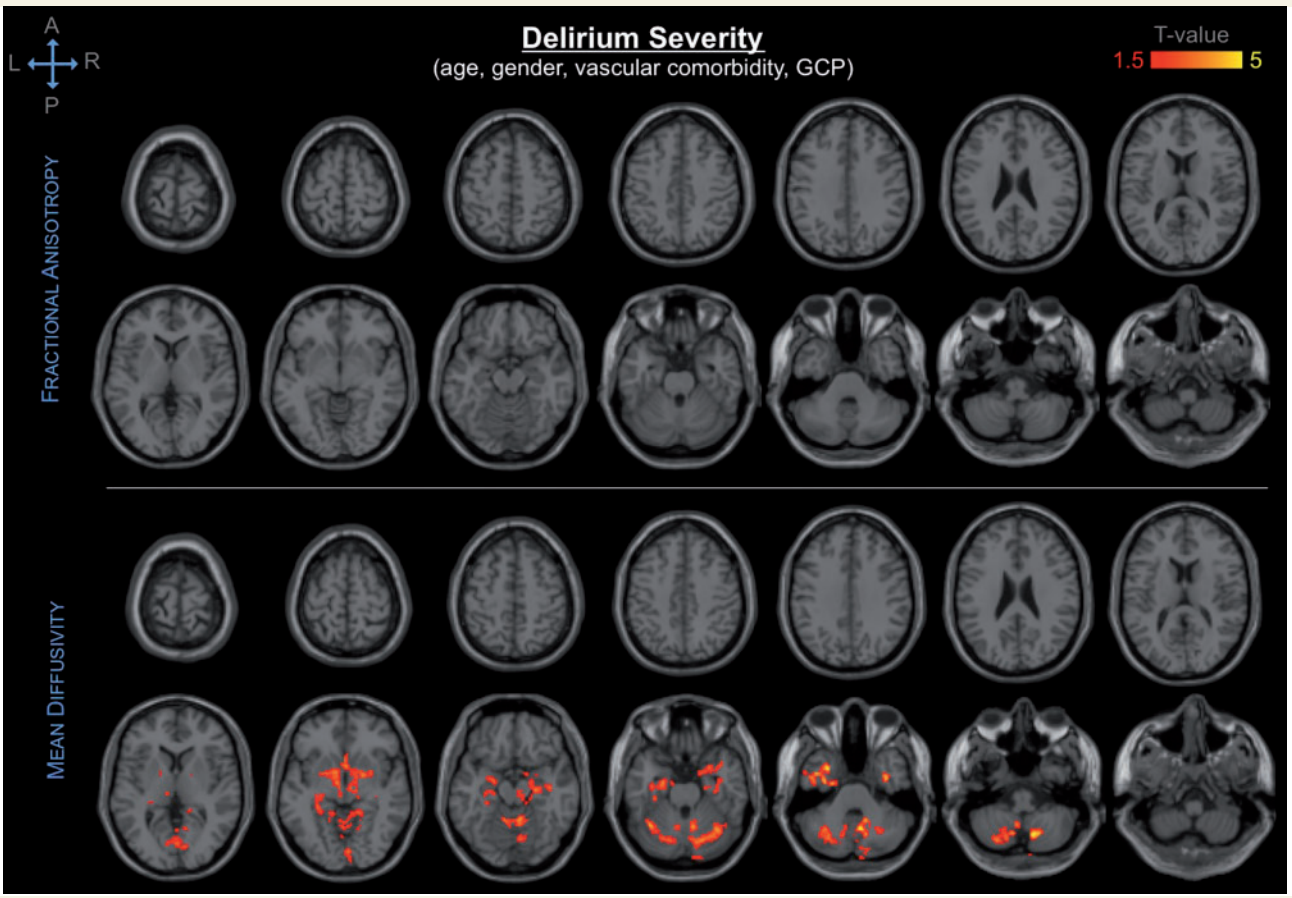

Figure 2 Spatial distribution and significance of association between DTI abnormalities and delirium severity, adjusting for age, gender, vascular comorbidity and GCP. Areas showing decrease in fractional anisotropy (*top*) and increase in mean diffusivity (*bottom*) are overlaid to canonical T_1-weighted images. Colours refer to T-values of significant DTI abnormalities ($P < 0.05$ after correction for multiple comparison within each cluster, cluster size $\geqslant 5000$) on a scale of 1.5 (red) to 5 (yellow).

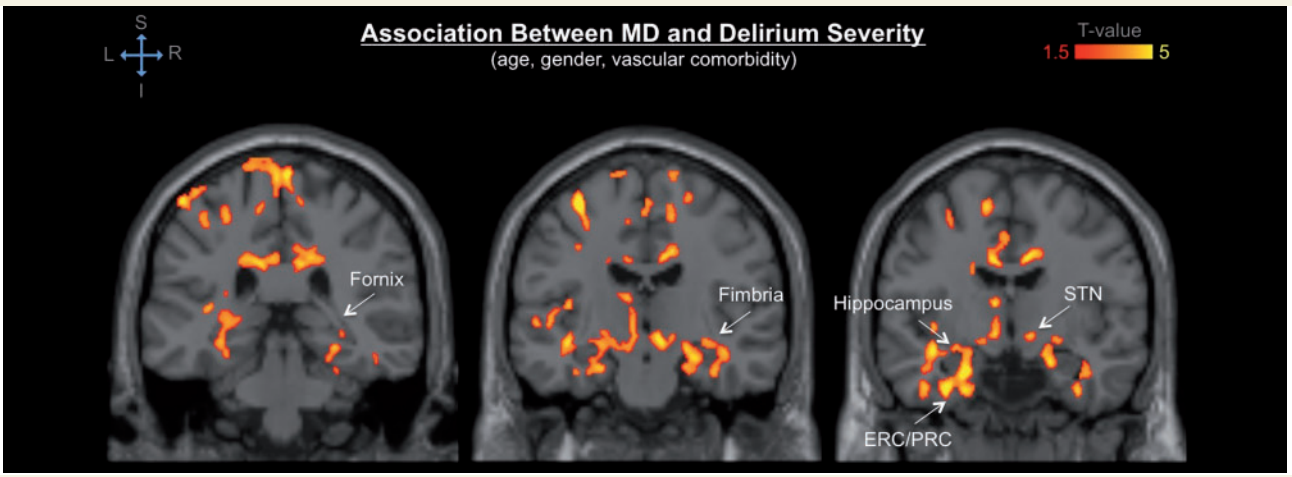

Figure 3 Anatomical detail of the DTI abnormalities of the temporal lobe associated with postoperative delirium. The colour map indicates significant association between regional mean diffusivity (MD) values and delirium severity in the bilateral temporal lobe, including hippocampal head and body, fimbria, and fornix, as well as entorhinal and perirhinal cortices (ERC/PRC). Significant associations are also noted in the subthalamic nucleus (STN) bilaterally and temporal stem white matter as well as dorsomedial thalamus. Colours refer to T-values of significant DTI abnormalities ($P < 0.05$ after correction for multiple comparison within each cluster, cluster size $\geqslant 5000$; general linear model adjusted for age, gender and vascular comorbidity) on a scale of 1.5 (red) to 5 (yellow).

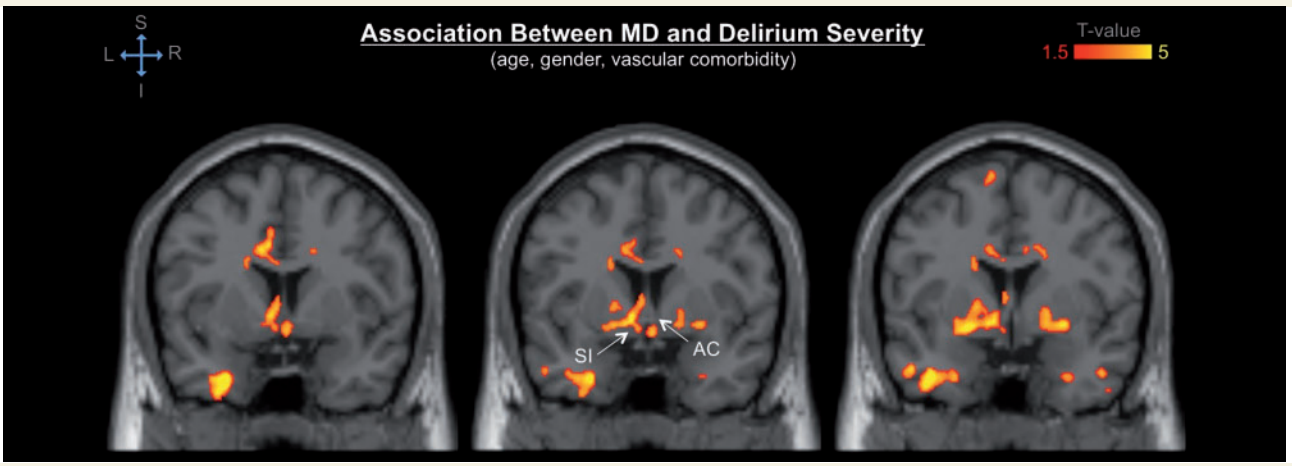

Figure 4 Detail of the DTI abnormalities of the basal forebrain associated with postoperative delirium. The colour map indicates significant association between regional mean diffusivity (MD) values and delirium severity in the bilateral substantia innominata (SI) and anterior commissure (AC). Colours refer to T-values of significant DTI abnormalities ($P < 0.05$ after correction for multiple comparison within each cluster, cluster size $\geqslant 5000$; general linear model adjusted for age, gender and vascular comorbidity) on a scale of 1.5 (red) to 5 (yellow).

Table 2 Summary of DTI abnormalities of the main brain structures associated with delirium incidence and severity

	Delirium incidence				Delirium severity			
	AD	FA	MD	RD	AD	FA	MD	RD
Cerebellum	*ns*	$\downarrow\downarrow^{L}$	$\uparrow^{*,R}$	$\uparrow\uparrow^{*,R}$	$\uparrow^{**,B}$	*ns*	$\uparrow^{**,B}$	$\uparrow^{**,B}$
Cingulum	*ns*	$\downarrow\downarrow^{B}$	*ns*	*ns*	$\uparrow^{B}$	$\downarrow\downarrow^{B}$	$\uparrow^{B}$	$\uparrow\uparrow^{B}$
Corpus callosum	*ns*	$\downarrow\downarrow$	$\uparrow$	$\uparrow\uparrow$	*ns*	$\downarrow\downarrow$	$\uparrow$	$\uparrow\uparrow$
Hippocampus	*ns*	*ns*	*ns*	*ns*	$\uparrow\uparrow^{**,L}$	*ns*	$\uparrow\uparrow^{**,B}$	$\uparrow\uparrow^{**,B}$
Internal capsule	*ns*	$\downarrow\downarrow^{L}$	*ns*	*ns*	*ns*	$\downarrow\downarrow^{L}$	$\uparrow\uparrow^{**,B}$	$\uparrow\uparrow^{*,L}$
Occipital lobe	*ns*	*ns*	*ns*	*ns*	*ns*	$\downarrow\downarrow^{R}$	*ns*	$\uparrow\uparrow^{B}$
Parietal lobe	*ns*	*ns*	*ns*	*ns*	*ns*	$\downarrow\downarrow^{R}$	$\uparrow^{R}$	$\uparrow^{R}$
Temporal lobe	*ns*	*ns*	*ns*	*ns*	$\uparrow\uparrow^{**,L}$	*ns*	$\uparrow\uparrow^{**,B}$	$\uparrow\uparrow^{**,B}$
Thalamus	*ns*	$\downarrow\downarrow^{L}$	*ns*	*ns*	$\uparrow\uparrow^{*,L}$	$\downarrow\downarrow^{B}$	$\uparrow\uparrow^{**,B}$	$\uparrow\uparrow^{**,B}$

$\uparrow$ Indicates significant increase in DTI metric associated with delirium outcome, controlling for age, gender, and vascular comorbidity with $P \leqslant 0.05$.
$\uparrow\uparrow$ Indicates significant increase in DTI metric associated with delirium outcome, controlling for age, gender, and vascular comorbidity with $P \leqslant 0.01$.
$\downarrow$ Indicates significant decrease in DTI metric associated with delirium outcome, controlling for age, gender, and vascular comorbidity with $P \leqslant 0.05$.
$\downarrow\downarrow$Indicates significant decrease in DTI metric associated with delirium outcome, controlling for age, gender, and vascular comorbidity with $P \leqslant 0.01$.
*Indicates significant association after adjustment for GCP in addition to age, gender, and vascular comorbidity with $P \leqslant 0.05$.
**Indicates significant association after adjustment for GCP in addition to age, gender, and vascular comorbidity with $P \leqslant 0.01$.
ns =No significant association between DTI metric and delirium outcome, controlling for age, gender, and vascular comorbidity.
L/R Indicates unilateral (left/right) DTI abnormalities of the structure of interest (bilateral structures only).
B Indicates bilateral DTI abnormalities of the structure of interest (bilateral structures only). AD = axial diffusivity; MD = mean diffusivity; RD = radial diffusivity; FA = fractional anisotropy.

broader spatial patterns of tissue abnormalities associated with delirium than axial diffusivity and fractional anisotropy. Results of the associations of all DTI indices with delirium incidence and severity are shown in Supplementary Figs 1–4, and summarized in Table 2.

We found no significant association between the DTI indices of the global cerebral white matter and delirium severity ($P \geqslant 0.2$; general linear model, adjusting for age, gender and disease duration).

GCP score was associated with a broad spatial pattern of DTI abnormalities of the frontal, temporal, parietal and occipital lobes, as well as of the thalamus and corpus callosum (Fig. 5 and Supplementary Fig. 5). Among these regions, the frontal white matter, temporal lobe (including the hippocampus), thalamus, and corpus callosum showed the most significant association with GCP.

Association between age and DTI abnormalities showed a widespread spatial pattern, including the frontal, parietal, occipital, and temporal white matter, as well as the thalamus and the cerebellum (Supplementary Fig. 6). The thalamus, internal capsule, frontal white matter, and hippocampus were the regions showing the most significant association between DTI signal abnormalities and age.

In supplementary analyses, we investigated the magnitude of the observed association between DTI abnormalities and delirium. Results showed mean differences in DTI indices

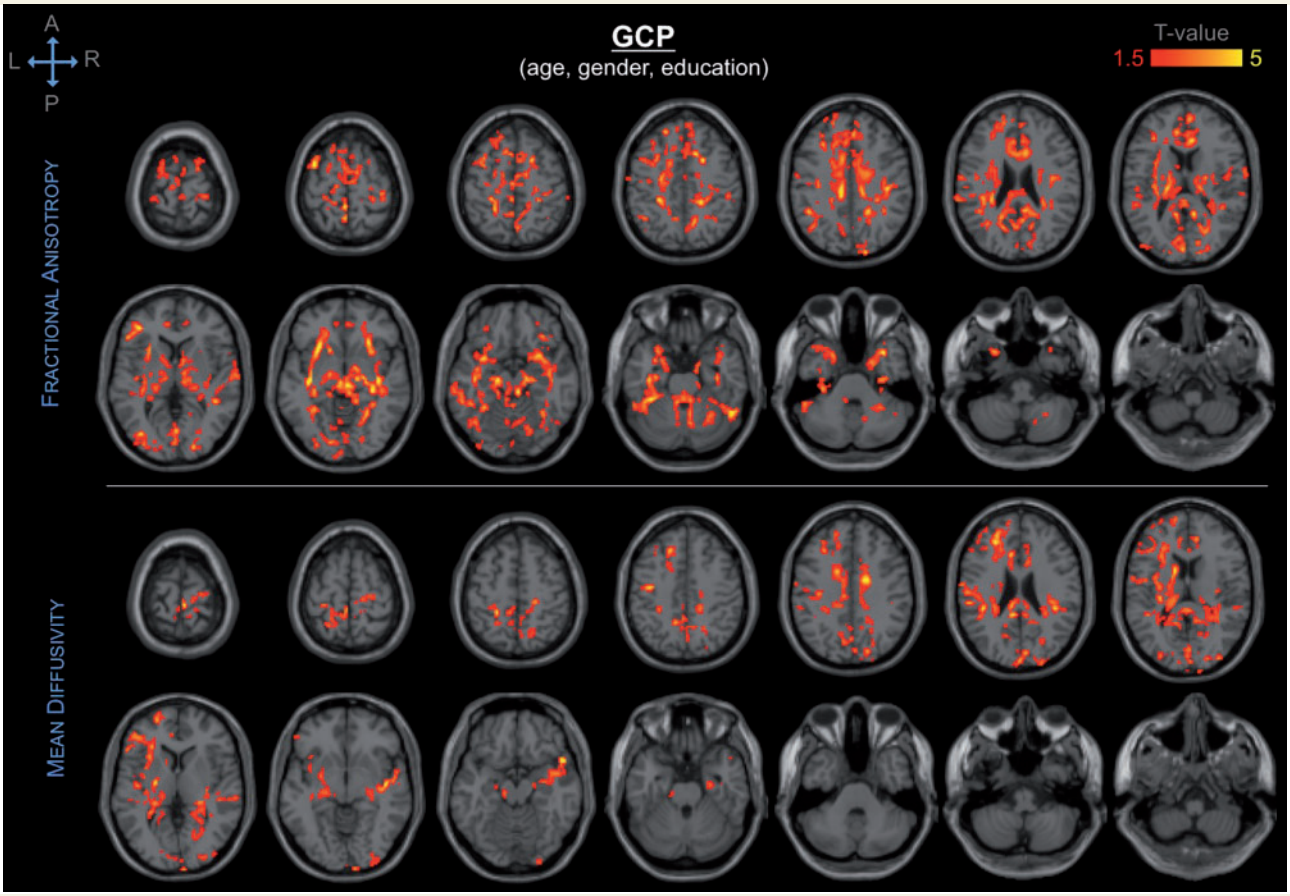

Figure 5 Spatial distribution and significance of association between DTI abnormalities and GCP, adjusting for age, gender and education. Areas showing decrease in fractional anisotropy (*top*) and increase in mean diffusivity (*bottom*) are overlaid to canonical T_1-weighted images. Colours refer to T-values of significant DTI abnormalities ($P < 0.05$ after correction for multiple comparison within each cluster, cluster size $\geqslant 5000$) on a scale of 1.5 (red) to 5 (yellow).

between delirium and non-delirium groups ranging from 3% to 8% (Table 3). Regression analysis showed significant association between DTI indices and delirium severity, adjusting for age, gender and vascular comorbidity, with standardized regression coefficients ranging from 0.4 to 0.7 (Supplementary Table 1 and Supplementary Fig. 7).

Discussion

Despite the significant impact of postoperative delirium on the prognosis and long-term outcome of older patients, its neural basis has not yet been clarified. By investigating regional brain abnormalities through DTI, our study aimed to provide insight into the neural substrate of delirium while controlling for other relevant predisposing factors, such as age, gender and vascular comorbidity. Our finding of an association of premorbid DTI abnormalities with delirium incidence and severity supports the hypothesis that structural dysconnectivity and microstructural tissue changes can predispose to delirium under the stress of surgery. DTI abnormalities are considered to reflect axonal degeneration and/or myelin loss in white matter tracts, as well as loss of microstructural integrity (e.g. gliosis, dendritic stripping), cell swelling or iron accumulation in grey matter structures at the histopathological level (Budde *et al.*, 2007; Hasan *et al.*, 2008). Our findings indicate that structural dysconnectivity involving the interhemispheric and fronto-thalamo-cerebellar networks, as well as microstructural changes of structures involved in limbic and memory functions are relevant neuroanatomical substrates of postsurgical delirium.

Postoperative delirium is the expression of a vulnerable brain that, under the stress of surgery, experiences cognitive and behavioural dysfunction, especially in activities related to attention. The spatial distribution of the delirium associated DTI abnormalities involves brain structures that are key connections and nodes of major brain networks including the frontoparietal control network (Vincent *et al.*, 2008) and the default mode network (Raichle *et al.*, 2001). One explanation for our findings is that pre-existing damage to the coordinated activity within attentional networks makes them more vulnerable to failure under stresses, such as surgery and hospitalization. Those subjects with such damage are consequently at enhanced risk for delirium.

Table 3 Mean axial-, mean- and radial diffusivity and fractional anisotropy differences between subjects with and without delirium in the brain regions showing significant association with delirium

DTI index	Region of interest	Cluster size	Delirium	No delirium	*P*-value
AD	Cingulum	5386	1.378 (0.106) × 10^{-3}	1.342 (0.059) × 10^{-3}	0.088
	Corpus callosum Left temporal lobe Left thalamus	11753	1.160 (0.091) × 10^{-3}	1.104 (0.063) × 10^{-3}	0.004
	Right temporal lobe Right parietal lobe	7898	1.372 (0.124) × 10^{-3}	1.310 (0.076) × 10^{-3}	0.015
FA	Cingulum Thalamus	18031	0.315 (0.026)	0.333 (0.023)	0.002
	Corpus callosum Right optic radiation	18343	0.353 (0.025)	0.370 (0.022)	0.002
MD	Cingulum Corpus callosum Left thalamus Left temporal lobe	31908	1.050 (0.094) × 10^{-3}	0.998 (0.053) × 10^{-3}	0.008
	Left frontal lobe Left parietal lobe	7535	0.857 (0.099) × 10^{-3}	0.807 (0.051) × 10^{-3}	0.013
	Left cerebellum	5150	0.798 (0.063) × 10^{-3}	0.756 (0.048) × 10^{-3}	0.002
	Right thalamus Right temporal lobe	7124	0.816 (0.086) × 10^{-3}	0.786 (0.061) × 10^{-3}	0.092
	Right parietal lobe	5748	0.706 (0.059) × 10^{-3}	0.661 (0.045) × 10^{-3}	0.001
	Right cerebellum Vermis	9206	1.059 (0.118) × 10^{-3}	1.017 (0.080) × 10^{-3}	0.080
RD	Cingulum Thalamus	38136	0.706 (0.059) × 10^{-3}	0.661 (0.045) × 10^{-3}	0.001
	Frontal lobe Parietal lobe	10820	0.894 (0.098) × 10^{-3}	0.838 (0.060) × 10^{-3}	0.006
	Left cerebellum	5872	0.804 (0.091) × 10^{-3}	0.741 (0.042) × 10^{-3}	0.001
	Right cerebellum	8320	0.785 (0.052) × 10^{-3}	0.729 (0.052) × 10^{-3}	0.001

Regions of interest correspond to the clusters that showed significant association with delirium severity in voxel-wise analysis (general linear model controlling for age, gender and vascular comorbidities). Cluster size is reported as number of voxels within each cluster. DTI indices are reported as mean (SD) within each cluster; fractional anisotropy is a scalar value between 0 and 1, the other DTI indices are expressed in mm^2/s. *P*-values refer to two-sided Student's *t*-test. AD = axial diffusivity; MD = mean diffusivity; RD = radial diffusivity; FA = fractional anisotropy.

The abnormalities of the corpus callosum could be linked to impairment in integrative functions observed in subjects with delirium (e.g. disorganized thinking). The finding is also consistent with previous case reports of transient signal abnormalities observed on T_2- and diffusion-weighted imaging in the corpus callosum in subjects with delirium (as reviewed in Alsop *et al.*, 2006).

The DTI abnormalities of the temporal lobe, hippocampus and cingulum are consistent with impairment in limbic, visuospatial and memory functions, which often characterize the delirium syndrome (e.g. disorientation, inability to learn or recall information, and perceptual abnormalities). In particular, the observed DTI abnormalities of the full circuit from entorhinal/perirhinal cortex, hippocampal head/body, and fimbria/fornix, which together represent the major outflow tract of the hippocampus, suggest that the abnormal integrity of the medial temporal lobe memory system is an important contributor to delirium severity (Fig. 3). Interestingly, while hippocampal volume was not significantly associated with delirium in our previous work on this cohort (Cavallari *et al.*, 2015), DTI measures appeared to be sensitive to detect hippocampal microstructural abnormalities in subjects with delirium. This finding is consistent with recent work on prodromal Alzheimer's disease, suggesting that compared to volumetrics, DTI measures of the hippocampus—especially mean- and radial diffusivity—are more sensitive correlates of cognitive impairment (Müller *et al.*, 2007; Carlesimo *et al.*, 2010; Zhang *et al.*, 2013). It is theoretically possible that the observed DTI abnormalities involving the hippocampal network reflect early Alzheimer's pathology, and therefore their association with delirium could be explained, at least in part, by the relationship between Alzheimer's disease and delirium (Inouye *et al.*, 2014). As this is an ongoing study, and we are still acquiring and analysing longitudinal cognitive data, it is not possible at present to investigate whether the observed hippocampal DTI abnormalities are associated with subsequent evolution to cognitive impairment or dementia in our study cohort. This will be a subject of future analysis.

The substantia innominata/basal forebrain is a major source of ascending cholinergic input to the cortex (e.g. neurons of the nucleus basalis of Meynert), critical to

arousal and attentional networks. The observed DTI abnormalities in these structures may account for the impaired level of arousability and responsiveness, as well as inattention observed in subjects with delirium.

Although the subthalamic nucleus has been traditionally regarded as a structure involved in motor control, recent work supported involvement of this structure in behavioural inhibition and impulsivity (Zavala *et al.*, 2015).

The observed DTI abnormalities of the anterior and dorsal 'shell' of the thalamus may indicate fronto-thalamic structural dysconnectivity (Schmahmann and Pandya, 2008), which underlie attentional and executive functions that are often impaired during delirium episodes (e.g. reduced ability to maintain and shift attention to external stimuli, and disorganized thinking associated with incoherent, tangential or circumstantial speech).

Among the structures with DTI signal abnormalities, the cerebellum showed the most prominent association with postoperative delirium. Although the cerebellum has been traditionally regarded as a motor structure involved in control of gait, balance, and voluntary movements, its involvement in cognitive and behavioural functions has been increasingly acknowledged. Cerebellar lesions with similar spatial distribution to the DTI abnormalities observed in our study—i.e. involving the vermis and posterior lobes—constitute the neuropathological substrate of the cerebellar cognitive affective syndrome, described in patients with cerebellar lesions (such as stroke, tumour and post-infectious cerebellitis) or cerebellar cortical atrophy (Schmahmann and Sherman, 1998). Similar to delirium, this syndrome is characterized by impaired ability to regulate or modulate cognitive function and behaviour in a manner appropriate to the context. Structural and functional cerebellar abnormalities have also been reported in other psychiatric disorders with attentional or executive impairment, such as schizophrenia, mood and attention deficit disorders, and autism (Schmahmann, 2004; Shakiba, 2014).

Of note, the subject excluded from this study due to failure of the registration algorithm developed delirium after surgery and showed MRI abnormalities that are qualitatively similar to the findings of voxel-wise DTI analyses. Specifically, conventional MRI sequences (T_1-weighted, T_2-weighted and FLAIR) of this study participant showed expanded retrocerebellar CSF space associated with cerebellar atrophy, and evidence of previous right temporal lobe stroke.

Age showed a widespread effect on the microstructure of both white matter connections and grey matter structures, including those that appeared to be relevant to delirium in our study. The findings suggest that age-related factors play a major role in the development of the DTI abnormalities observed in subjects with delirium. However, the observed spatial distribution of the DTI abnormalities associated with age is quite different from the delirium-associated pattern. This finding, together with the lack of significant association between global white matter DTI indices and delirium, support the regional specificity of the observed microstructural abnormalities associated with delirium.

When comparing the DTI values between the subjects with delirium and those without in supplementary analysis, we found significant decrease in fractional anisotropy, as well as increase in axial-, mean- and radial diffusivity in a variety of brain regions (Table 3). While these measures of premorbid microstructural abnormalities were associated with an increased risk of developing delirium after surgery, the magnitude of the observed differences between the groups does not seem to be immediately translatable into plans for individual risk assessment and management in clinical settings. The definition of the regions of interest, based on heuristic observation of DTI abnormalities in brain areas that were then compared and probed as predictors of delirium in the regression analysis rather than on *a priori* hypothesis, may explain the strong association between DTI indices and delirium observed in the regions of interest analysis (Supplementary Table 1).

Our findings are consistent with previous DTI studies of delirium, which showed an association between premorbid changes of the frontal white matter and thalamus with postoperative delirium, which occurred in 19 of 116 study subjects after cardiac surgery (Shioiri *et al.*, 2010), as well as an inverse association of fractional anisotropy of the internal capsule and corpus callosum at discharge MRI scan with delirium duration in 47 intensive care unit patients (Morandi *et al.*, 2012). In both studies only fractional anisotropy analysis was performed. In addition, those previous studies present limitations related to the lack of premorbid MRI assessment (Morandi *et al.*, 2012), as well as clinically relevant age differences between subjects with and without delirium, and potential methodological pitfalls regarding image co-registration (Shioiri *et al.*, 2010). Our results are based on the largest prospectively acquired sample analysed thus far to assess the association between premorbid DTI abnormalities and delirium. The multidimensional, comprehensive assessment of clinical variables within the SAGES study enabled us to control for potential confounders, and to investigate the relationship between premorbid microstructural connection abnormalities and cognitive performance in subjects with postoperative delirium. In addition, our DTI measures rely on improved image co-registration to ensure alignment across the individual images. By analysing multiple DTI indices (axial-, mean- and radial diffusivity, in addition to fractional anisotropy) we were able to detect a much larger effect of microstructural brain abnormalities on delirium, which involved structures that were not previously shown to be associated with postoperative delirium.

Analysis of the relationship between DTI abnormalities, cognitive status and postoperative delirium allowed us to distinguish between two pathological phenomena, which diverged in their dependence from GCP. Cognitive function is an established predisposing factor for postoperative delirium (Rudolph *et al.*, 2007; Inouye *et al.*, 2014), and we found an association of GCP score before surgery with delirium incidence and severity in our study population of cognitively normal individuals (Cavallari *et al.*, 2015). DTI abnormalities of the

cingulum, corpus callosum, occipital, parietal and temporal lobes were associated with postoperative delirium when controlling for age, gender and vascular comorbidity, but not when controlling also for GCP (Figs 1 and 2). These findings, together with the consistent spatial pattern of association between DTI signal and GCP (Fig. 5), suggest that the DTI abnormalities observed in those structures constitute the neural substrate for the association between presurgical cognitive impairment and postoperative delirium. Interestingly, DTI changes involving the cerebellum, hippocampus, basal forebrain and part of the thalamus, appeared to be associated with delirium incidence and severity, independently from cognitive status, as measured by GCP before surgery. Although DTI abnormalities of these structures seems to play a major role in the development of postoperative delirium, we cannot rule out possible involvement of widespread damage across more distributed networks, which might not have shown significant association with delirium due to limited spatial specificity.

The association between DTI abnormalities and delirium severity was overall more significant and showed a broader spatial pattern compared to delirium incidence. This result likely reflects the nature of delirium as a spectrum disorder characterized by a continuum between no symptoms and delirium syndrome as defined by the full CAM algorithm. In dichotomizing presence/absence of delirium, inclusion of subjects with subsyndromal delirium in the group of patients without delirium may have biased some of the results towards the null hypothesis (i.e. no association between DTI indices and delirium).

We acknowledge a number of limitations of this study. Generalizability of our findings is limited as our study included only older subjects with no evidence of dementia, and was based on an elective surgical population in a single geographic area. Future studies will be needed to verify the findings in other settings, such as general medicine, intensive care, and post-acute settings, and other populations, such as subjects with dementia. In prioritizing adjustment for relevant baseline covariables, we could not account for other potential confounders, such as factors related to the surgical experience. This study examined only the role of presurgical DTI biomarkers for the prediction of delirium. Interesting lines of future research include longitudinal assessment of DTI changes in subjects with postoperative delirium, and their relationship with cognitive decline over time. Future DTI studies using more advanced acquisition (e.g. multi-band parallel EPI acquisition, multi b-value diffusion spectrum imaging) and analysis approaches (e.g. tractography) are also warranted to improve the anatomical detail of the observed association between DTI abnormalities and delirium.

The neuroanatomical substrates of delirium remain largely elusive due to the multiple factors involved in the pathogenesis of delirium. This study raises the intriguing possibility that disruptions in interhemispheric, fronto-thalamo-cerebellar, limbic and memory networks constitute the neural basis of delirium. While the DTI abnormalities observed in the corpus callosum, cingulum, and temporal white matter likely reflect regional brain damage that underlies the association between premorbid cognitive function and postoperative delirium, the microsctructural changes observed in the cerebellum, hippocampus, basal forebrain and part of the thalamus seems to constitute a phenomenon that predisposes to postsurgical delirium independent of baseline cognitive performance.

Acknowledgements

A list of participating personnel of the SAGES Study can be found online as Supplementary material.

Funding

Supported by Grants No. P01AG031720 (S.K.I.) and K07AG041835 (S.K.I.) from the National Institute on Aging. T.T.H. is supported by a NIH funded T32 Training Grant (AG000158). E.R.M. is supported by K24AG035075 from the National Institute on Aging. S.K.I. holds the Milton and Shirley F. Levy Family Chair. The funding sources had no role in the design, conduct, or reporting of this study.

Supplementary material

Supplementary material is available at *Brain* online.

References

Alsop DC, Fearing MA, Johnson K, Sperling R, Fong TG, Inouye SK. The role of neuroimaging in elucidating delirium pathophysiology. J Gerontol A Biol Sci Med Sci 2006; 61: 1287–93.

Brandt J. The hopkins verbal learning test: development of a new memory test with six equivalent forms. Clin Neuropsychol 1991; 5: 125–42.

Brett M, Anton JL, Valabregue R, Poline JB. Region of interest analysis using an SPM toolbox. In: Presented at the 8th International Conference on Functional Mapping of the Human Brain, Sendai, Japan, 2002. Available in Neuroimage 16: 2.

Budde MD, Kim JH, Liang HF, Schmidt RE, Russell JH, Cross AH, et al. Toward accurate diagnosis of white matter pathology using diffusion tensor imaging. Magn Reson Med 2007; 57: 688–95.

Carlesimo GA, Cherubini A, Caltagirone C, Spalletta G. Hippocampal mean diffusivity and memory in healthy elderly individuals: a cross-sectional study. Neurology 2010; 74: 194–200.

Cavallari M, Hshieh TT, Guttmann CRG, Ngo LH, Meier DS, Schmitt EM, et al. Brain atrophy and white matter hyperintensities are not significantly associated with incidence and severity of postoperative delirium in older persons without dementia. Neurobiol Aging 2015; 36: 2122–9.

Friston KJ, Worsley KJ, Frackowiak RS, Mazziotta JC, Evans AC. Assessing the significance of focal activations using their spatial extent. Hum Brain Mapp 1994; 1: 210–20.

Glymour M, Greenland S. Causal diagrams. In: Rothman K, Greenland S, Lash T, editors. Modern Epidemiology. 3d. Philadelphia, PA: Lippincott Williams & Wilkins; 2008. pp. 183–209

Griffa A, Baumann PS, Thiran JP, Hagmann P. Structural connectomics in brain diseases. Neuroimage 2013; 80: 515–26.

Gross AL, Jones RN, Fong TG, Tommet D, Inouye SK. Calibration and validation of an innovative approach for estimating general cognitive performance. Neuroepidemiology 2014; 42: 144–53.

Gunther ML, Morandi A, Krauskopf E, Pandharipande P, Girard TD, Jackson JC, et al. The association between brain volumes, delirium duration, and cognitive outcomes in intensive care unit survivors: the VISIONS cohort magnetic resonance imaging study*. Crit Care Med 2012; 40: 2022–32.

Hasan KM, Halphen C, Boska MD, Narayana PA. Diffusion tensor metrics, T2 relaxation, and volumetry of the naturally aging human caudate nuclei in healthy young and middle-aged adults: possible implications for the neurobiology of human brain aging and disease. Magn Reson Med 2008; 59: 7–13.

Hatano Y, Narumoto J, Shibata K, Matsuoka T, Taniguchi S, Hata Y, et al. White-matter hyperintensities predict delirium after cardiac surgery. Am J Geriatr Psychiatry 2013; 21: 938–45.

Inouye SK, Bogardus ST, Charpentier PA, Leo-Summers L, Acampora D, Holford TR, et al. A multicomponent intervention to prevent delirium in hospitalized older patients. N Engl J Med 1999; 340: 669–76.

Inouye SK, van Dyck CH, Alessi CA, Balkin S, Siegal AP, Horwitz RI. Clarifying confusion: the confusion assessment method: a new method for detection of delirium. Ann Intern Med 1990; 113: 941–8.

Inouye SK, Kosar CM, Tommet D, Schmitt EM, Puelle MR, Saczynski JS, et al. The CAM-S: development and validation of a new scoring system for delirium severity in 2 cohorts. Ann Intern Med 2014; 160: 526–33.

Inouye SK, Leo-Summers L, Zhang Y, Bogardus ST, Leslie DL, Agostini JV. A chart-based method for identification of delirium: validation compared with interviewer ratings using the confusion assessment method. J Am Geriatr Soc 2005; 53: 312–8.

Inouye SK, Westendorp RGJ, Saczynski JS. Delirium in elderly people. Lancet 2014; 383: 911–22.

Jones RN, Rudolph JL, Inouye SK, Yang FM, Fong TG, Milberg WP, et al. Development of a unidimensional composite measure of neuropsychological functioning in older cardiac surgery patients with good measurement precision. J Clin Exp Neuropsychol 2010; 32: 1041–9.

Keihaninejad S, Zhang H, Ryan NS, Malone IB, Modat M, Cardoso MJ, et al. NeuroImage An unbiased longitudinal analysis framework for tracking white matter changes using diffusion tensor imaging with application to Alzheimers' disease. Neuroimage 2013; 72: 153–63.

Mack WJ, Freed DM, Williams BW, Henderson VW. Boston naming test: shortened versions for use in Alzheimer's disease. J Gerontol 1992; 47: P154–8.

Marcantonio ER, Flacker JM, Wright RJ, Resnick NM. Reducing delirium after hip fracture: a randomized trial. J Am Geriatr Soc 2001; 49: 516–22.

Marcantonio ER, Kiely DK, Simon SE, John Orav E, Jones RN, Murphy KM, et al. Outcomes of older people admitted to postacute facilities with delirium. J Am Geriatr Soc 2005; 53: 963–9.

Milisen K, Foreman MD, Abraham IL, De Geest S, Godderis J, Vandermeulen E, et al. A nurse-led interdisciplinary intervention program for delirium in elderly hip-fracture patients. J Am Geriatr Soc 2001; 49: 523–32.

Morandi A, Rogers BP, Gunther ML, Merkle K, Pandharipande P, Girard TD, et al. The relationship between delirium duration, white matter integrity, and cognitive impairment in intensive care unit survivors as determined by diffusion tensor imaging: the VISIONS prospective cohort magnetic resonance imaging study*. Crit Care Med 2012; 40: 2182–9.

Müller MJ, Greverus D, Weibrich C, Dellani PR, Scheurich A, Stoeter P, et al. Diagnostic utility of hippocampal size and mean diffusivity in amnestic MCI. Neurobiol Aging 2007; 28: 398–403.

Pierpaoli C, Jezzard P, Basser PJ, Barnett A, Di Chiro G. Diffusion tensor MR imaging of the human brain. Radiology 1996; 201: 637–48.

Quinlan N, Rudolph JL. Postoperative delirium and functional decline after noncardiac surgery. J Am Geriatr Soc 2011; 59 (Suppl 2): S301–4.

Raichle ME, MacLeod AM, Snyder AZ, Powers WJ, Gusnard DA, Shulman GL. A default mode of brain function. Proc Natl Acad Sci USA 2001; 98: 676–82.

Root JC, Pryor KO, Downey R, Alici Y, Davis ML, Holodny A, et al. Association of pre-operative brain pathology with post-operative delirium in a cohort of non-small cell lung cancer patients undergoing surgical resection. Psychooncology 2013; 22: 2087–94.

Rudolph JL, Jones RN, Rasmussen LS, Silverstein JH, Inouye SK, Marcantonio ER. Independent vascular and cognitive risk factors for postoperative delirium. Am J Med 2007; 120: 807–13.

Saczynski JS, Kosar CM, Xu G, Puelle MR, Schmitt E, Jones RN, et al. A tale of two methods: chart and interview methods for identifying delirium. J Am Geriatr Soc 2014; 62: 518–24.

Saczynski JS, Marcantonio ER, Quach L, Fong TG, Gross A, Inouye SK, et al. Cognitive trajectories after postoperative delirium. N Engl J Med 2012; 367: 30–9.

Sasson E, Doniger GM, Pasternak O, Tarrasch R, Assaf Y. Structural correlates of cognitive domains in normal aging with diffusion tensor imaging. Brain Struct Funct 2012; 217: 503–15.

Schisterman EF, Cole SR, Platt RW. Overadjustment bias and unnecessary adjustment in epidemiologic studies. Epidemiology 2009; 20: 488–95.

Schmahmann JD, Pandya DN. Disconnection syndromes of basal ganglia, thalamus, and cerebrocerebellar systems. Cortex 2008; 44: 1037–66.

Schmahmann JD, Sherman JC. The cerebellar cognitive affective syndrome. Brain 1998; 121: 561–79.

Schmahmann JD. Disorders of the cerebellum: ataxia, dysmetria of thought, and the cerebellar cognitive affective syndrome. J Neuropsychiatry Clin Neurosci 2004; 16: 367–78.

Schmitt EM, Marcantonio ER, Alsop DC, Jones RN, Rogers SO, Fong TG, et al. Novel risk markers and long-term outcomes of delirium: the successful aging after elective surgery (SAGES) study design and methods. J Am Med Dir Assoc 2012; 13: 818.e1–10.

Shakiba A. The role of the cerebellum in neurobiology of psychiatric disorders. Neurol Clin 2014; 32: 1105–15.

Shioiri A, Kurumaji A, Takeuchi T, Matsuda H, Arai H, Nishikawa T. White matter abnormalities as a risk factor for postoperative delirium revealed by diffusion tensor imaging. Am J Geriatr Psychiatry 2010; 18: 743–53.

Thomason ME, Thompson PM. Diffusion imaging, white matter, and psychopathology. Annu Rev Clin Psychol 2011; 7: 63–85.

Trail making tests A and B. Washington, DC: War Department, Adjutant General's Office; 1944.

Trenerry M, Crosson B, DeBoe J, Leber W. Visual Search and Attention Test (VSAT). Odessa, FL: Psychological Assessment Resources, Inc.; 1990.

Vincent JL, Kahn I, Snyder AZ, Raichle ME, Buckner RL. Evidence for afrontoparietal control system revealed by intrinsic functional connectivity. J Neurophysiol 2008; 100: 3328–42.

Wechsler D. Manual: wechsler adult intelligence scale - revised. New York: Psychological Corp; 1981.

Wei LA, Fearing MA, Sternberg EJ, Inouye SK. The confusion assessment method: a systematic review of current usage. J Am Geriatr Soc 2008; 56: 823–30.

Yendiki A, Panneck P, Srinivasan P, Stevens A, Zöllei L, Augustinack J, et al. Automated probabilistic reconstruction of white-matter pathways in health and disease using an atlas of the underlying anatomy. Front Neuroinform 2011; 5: 23.

Zavala B, Zaghloul K, Brown P. The subthalamic nucleus, oscillations, and conflict. Mov Disord 2015; 30: 328–38.

Zhang Y, Schuff N, Camacho M, Chao LL, Fletcher TP, Yaffe K, et al. MRI markers for mild cognitive impairment: comparisons between white matter integrity and gray matter volume measurements. PLoS One 2013; 8: e66367.